

# Mitigating exhalation puffs during oxygen therapy for respiratory disease

Arshad Kudrolli,<sup>1, a)</sup> Brian Chang,<sup>1</sup> Jade Consalvi,<sup>1</sup> Anton Deti,<sup>1</sup> Christopher Frechette,<sup>2</sup> Helen Scoville,<sup>2</sup> Geoffrey R. Sheinfeld,<sup>3</sup> and William T. McGee<sup>2</sup>

<sup>1)</sup>Department of Physics, Clark University, Worcester, MA 01610.

<sup>2)</sup>University of Massachusetts Medical School - Baystate, Springfield, MA 01107.

<sup>3)</sup>PO Box 459, Andover, MA 01810.

(Dated: March 30, 2022)

We investigate the dispersal of exhalations corresponding to a patient experiencing shortness of breath while being treated for respiratory disease with oxygen therapy. Respiration through a nasal cannula and a simple O<sub>2</sub> mask are studied using a supine manikin equipped with a controllable mechanical lung by measuring aerosol density and flow with direct imaging. Exhalation puffs are observed to travel  $0.35 \pm 0.02$  m upward while wearing a nasal cannula, and  $0.29 \pm 0.02$  m laterally through a simple O<sub>2</sub> mask, posing a higher direct exposure risk to caregivers. The aerosol-laden air flows were found to concentrate in narrow conical regions through both devices at several times their concentration level compared with a uniform spreading at the same distance. We test a mitigation strategy by placing a surgical mask loosely over the tested devices. The mask is demonstrated to alleviate exposure by deflecting the exhalations from being launched directly above a supine patient. The surgical mask is found to essentially eliminate the concentrated aerosol regions above the patient over the entire oxygenation rates used in treatment in both devices.

## I. INTRODUCTION

Oxygen therapy is the major treatment modality for patients with COVID-19 and other respiratory diseases who have low blood oxygen levels<sup>1,2</sup>. Depending on the severity of the condition, supplementary oxygen is delivered with various devices including a nasal cannula or a simple O<sub>2</sub> mask at the primary level, and more intensive treatment with high flow nasal cannula and the continuous positive airway pressure therapy, and finally at the most advanced level with full ventilatory support with endotracheal intubation<sup>1</sup>. While more intensive methods are administered in highly controlled clinical settings, the nasal cannula and the simple O<sub>2</sub> mask are used all over the world not only in clinical settings, but also at home and assisted care facilities. Further, these primary devices are used to provide supplementary oxygen during transportation to healthcare points, in waiting areas, and other improvised locations when healthcare support is stressed, such as during the current COVID-19 pandemic.

It is well known that the exhalations from subjects with respiratory disease can carry virus-laden aerosols which may infect healthy individuals depending on their distance and duration of exposure<sup>3</sup>. A typical adult exhales on average 5-6 liters of air per

minute while breathing normally with a tidal volume of approximately 500 mL at 12 breaths per minute, or with a lower tidal volume and higher compensatory breaths per minute while experiencing shortness of breath<sup>4,5</sup>. Pressurized tanks are used to deliver oxygen through an oxygenation device at a similar, if not higher, flow rate. Such noninvasive treatments, however, raise the possibility of greater dispersal distances of infected aerosols, which increases the risk to caregivers due to the corresponding increase of air flow near the patient.

Indeed, bioaerosol-laden exhalations through high flow oxygenation devices and its impact on infectious disease spread have been studied<sup>6,7</sup>, and informed early strategies used in treating COVID-19 patients by intubation because it allows sealed air pathways and minimal exhalation dispersal in the vicinity of the patient<sup>8</sup>. Poor outcomes following intubation have driven patient care to less invasive oxygen therapy, but by protecting clinicians and other caregivers with personal protection equipment (PPE) to minimize aerosol inhalation with N95 and medical masks<sup>8,9</sup>. Clinically, it is assumed that surgical face masks suffice for prevention of viral transmission from respiratory droplets, while N95 respirators provide additional protection from airborne transmission via bioaerosols<sup>10,11</sup>.

A significant body of work is being developed by analyzing the dispersal of aerosols and larger droplets over a range of exhalations resulting from activities such as talking, singing, sneezing or coughing<sup>12-15</sup>,

<sup>a)</sup>Electronic mail: akudrolli@clarku.edu (Corresponding author).

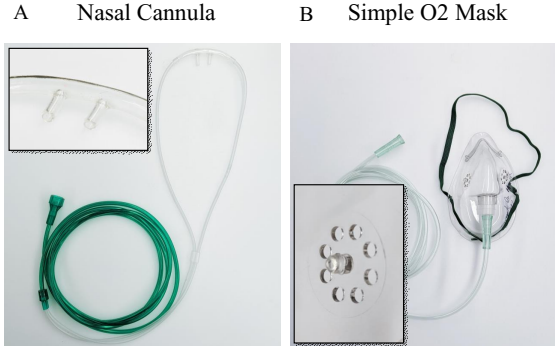


Figure 1. Images of the oxygenation devices used in the study (A,B). The nasal cannula is a tube that splits into two prongs that are partially inserted into the nose. The simple O<sub>2</sub> mask is a mask that covers both the nose and mouth with a tube that delivers the oxygen. Insets show closeup of the prongs in the nasal cannula (A), and the ventilation holes in the Simple O<sub>2</sub> mask (B).

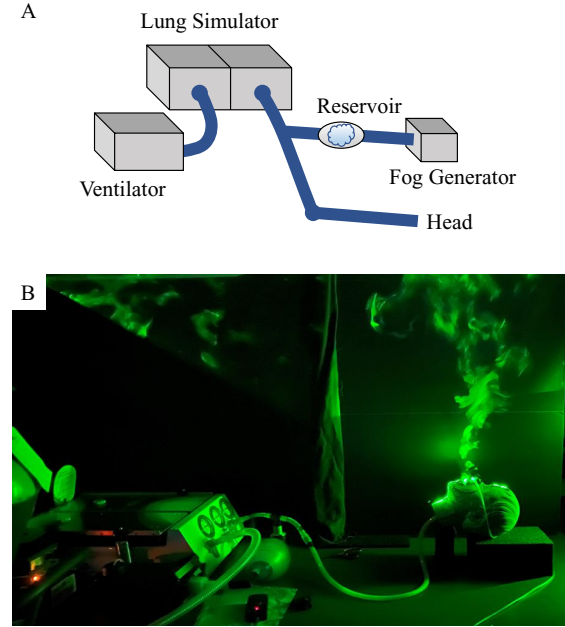


Figure 2. A: The study apparatus consists of a dual lung simulator driven by a ventilator coupled with a second lung chamber which “breathes” air through the manikin head shown with a prescribed frequency and tidal volume. B: Image of system with laser-sheet lighting used for aerosol visualization. The exhalations are visualized using water-glycerol aerosols (fog) released through the manikin mouth and/or nose during exhalation.

and mask mitigation to reduce exposure<sup>16–18</sup>. Several recent studies have utilized computational fluid dynamics to explore exhalations in terms of more detailed flow structures and complex scenarios<sup>19–22</sup>. Nonetheless, there is still a poor understanding of the physical characterization of exhalation dispersal while breathing under shortness of breath conditions, as experienced by infected patients. This understanding is still necessary because infections to health care workers remains a significant concern<sup>23,24</sup> during the current pandemic where health care facilities and PPEs are less than optimal, and particularly with new infectious variants of the SARS-CoV-2 virus. Indeed, COVID-19 - along with Severe acute respiratory syndrome (SARS), Influenza A (H1N1), Middle East Respiratory Syndrome (MERS), and Ebola - is one of 5 major respiratory infectious diseases to emerge in just the last 20 years alone.

Exhalation dispersal mitigation by a surgical mask over high flow oxygen therapy has been proposed<sup>25</sup> and preliminary clinical data is available for mitigation of aerosols close to the patient where bedside care is delivered<sup>26,27</sup>. The relative placement of a mask in the case of a patient receiving supplemental oxygen has been recently discussed<sup>28,29</sup>, but a clear demonstration of mask efficacy when worn by patients using commonly used oxygen delivery devices remains unclear and is not practiced widely<sup>30</sup>. Exhalation puffs - periodic turbulent exhalations with significant linear momentum and energy<sup>13,31</sup> - emerging from masks with vents are documented<sup>16</sup>, but hospitalized COVID-19 patients receiving oxygen rarely use further mitigation strategies. Evidence for var-

ious comparisons about masks used in health care settings and the associated risk for COVID-19 remains insufficient<sup>32</sup>. Any added risk posed by patients while being treated with a nasal canula and simple O<sub>2</sub> mask remains less appreciated.

In this study, we investigate the exhalations corresponding to a simulated patient being treated with a primary oxygenation device. The dispersal volume and density of the exhaled aerosol are visualized and characterized over space and time. We then demonstrate that a loosely placed surgical mask over a nasal cannula, or simple O<sub>2</sub> mask, decreases and redirects exhalations downward, and thus away from the faces of caregivers. The surgical mask is only loosely placed in our mitigation strategy to alleviate any concern for increased work of breathing.

## II. METHODS

We examine two commonly used oxygenation devices: the nasal cannula and the simple O<sub>2</sub> mask,

Oxygenation Device	Flow Rate $Q$ (Lpm)	Tidal Volume $V_t$ (mL)	Rate $f$ (bpm)
None	-	350	20
Nasal Cannula	0, 2, 4, 8	350	20
Simple O <sub>2</sub>	0, 4, 8, 12	350	20
Nasal Cannula	2	500	12
Simple O <sub>2</sub>	4	500	12

Table I. Summary of the oxygenation devices, flow rates in liters per minute (Lpm), and breathing tidal cycles in breaths per minute (bpm) investigated ( $Q = 0$  Lpm cases were conducted for calibration purposes).

shown in Fig. 1. The nasal cannula is a tube that splits into two prongs that are partially inserted into the nose. Oxygen is then delivered through the nose at a prescribed flow rate  $Q$  ranging between 2 Lpm and 8 Lpm (see Table. I). The simple O<sub>2</sub> mask covers both the nose and mouth of the patient, but has two vents that would allow air to freely pass in and out of the mask. Meanwhile, a steady oxygen supply is delivered through the mask at a rate of  $Q$  ranging between 4 Lpm and 12 Lpm. Such values are commonly used in practice for patients undergoing respiratory therapy<sup>5</sup>.

We developed a manikin respiration system which enables us to visualize and quantify the direction and density of aerosol-laden exhalations of patients being treated with oxygen therapy under prescribed and reproducible conditions. A schematic and image of our experimental apparatus is shown in Fig. 2. A Michigan Instruments Dual Lung Simulator and a ventilator (ParaPAC plus 310) are configured to mimic negative pressure patient respiration with a prescribed tidal volume and frequency. A tube connects the Lung Simulator with a Head Simulator Module (HSM-A), where the manikin is modified to breath through the nose and/or mouth. A tidal volume of  $V_t = 500$  mL with a breathing rate of  $f = 12$  breaths per minute (bpm) represents normal breathing. Patients that require oxygen assistance typically have a lower tidal volume which is compensated with a higher frequency<sup>4</sup>. Thus, a tidal volume of  $V_t = 350$  mL and respiratory rate of  $f = 20$  bpm simulated a patient with lung disease, and models typical COVID-19 patients who are experiencing shortness of breath while undergoing supplemental oxygen therapy.

Metered O<sub>2</sub> from a pressurized tank is delivered through a nasal cannula (Vyaire Medical Inc.) or a simple O<sub>2</sub> mask (Vyaire Medical Inc.) with flow rates,  $Q$ , listed in Table 1. Such flow rates are typically used in treating Covid-19 and other respiratory disease patients. All measurements were conducted

in a room with HVAC at 23.5°C with standard deviation of 0.5°C, and humidity 21.0% with standard deviation of 2.5 %. Such HVAC conditions are within range of standard OSHA regulations, which prescribe that indoor temperatures should remain within 20-24°C and relative humidity remain within 20-60%<sup>33,34</sup>.

In order to image the exhalations, we use an aerosol fog composed of approximately 1-5 micron water-based droplets which scatter light while moving with the air flows<sup>6,14</sup>. While the droplet sizes are optimized for light scattering and are more numerous, they are known to be within the size range of bioaerosols exhaled while breathing<sup>6,35,36</sup>.

Two complementary lighting methods are used to obtain the overall direction and spread of the aerosol-laden exhalations. This helps inform and deduce when the flows are puff-like with linear momentum, versus spreading diffusively as they slow down. We place a 5500 lumen LED white light source behind the head to backlight the aerosols in the exhalations<sup>12,15</sup>. All of the image analysis is conducted on the back-light videos. Additionally, we use a green laser sheet (532 nm, 40 mW) to visualize the flow in a 2D plane which helps qualitatively clarify flow structures<sup>13</sup>. A Pixel 4a smartphone camera is used to capture movies with 1080p at 30 frames per second (fps) over several exhalation cycles. All quantitative analysis is performed with at least 5 trials for each set of parameters. Time-averages of the exhalations  $\mu_t$  are obtained as  $\mu_t = \frac{1}{N} \sum_{t=1}^N I(x, y, t)$ , where  $I(x, y, t)$  is the 2-dimensional image with intensity values corresponding to each  $x$  and  $y$  pixel at frame  $t$ , and  $N$  is the number of frames.

An aerosol-laden air flow emerging from the nose of the manikin while free breathing and imaged with laser illumination is shown in Fig. 2B. The shape of the exhalation puff from the nose and mouth of the manikin is observed to be typical of a fast moving fluid exiting a nozzle and losing momentum in a quiescent-fluid<sup>37,38</sup>. Tracking the leading edge of

an exhalation puff over consecutive frames, we observed nasal exhalations with a speed of  $1.21 \pm 0.07$  m/s (mean  $\pm$  SD), consistent with the 0.4 to 1.6 m/s range reported for normal human nasal breathing<sup>36</sup>. These ranges of measured speeds were found to be also consistent with complementary tests conducted with a TES 1341 Hot-Wire Anemometer. The exhalation flow speed is observed to decrease below 0.01 m/s, corresponding to the ambient fluctuations in the room, at about 40-45 cm from the nozzles using this device.

### III. RESULTS

#### A. Dispersal through Nasal Cannula

Figure 3 shows time-averaged exhalations emerging from the manikin while undergoing oxygenation treatment with a nasal cannula under varying conditions over a time window of five exhalation cycles each (roughly 6 seconds per exhalation cycle). The corresponding movies can be found in Fig. 3 (Multimedia view). In each case a primary puff can be observed clearly extending from the nose past the nasal cannula as it enters and spreads conically in the relatively still-air in the room while losing speed. A nasal cannula typically only has one major puff coming directly from the nose. But, there are examples in which the stem of the nasal cannula may reflect the exhaled air up past the nose and over the head, as seen in SI Movie 2. We observe that the exhalation air flow on average emerges from the nose somewhat similarly in relation to the face, no matter its angle of tilt, i.e., the direction of the exhalation puff is essentially set by the direction of the face, as shown in Fig. 3A,B.

While wearing a nasal cannula, a speed of  $1.2 \pm 0.15$  cm/s is observed near the nose, and a distance of  $0.35 \pm 0.02$  m is reached before the exhalation puff loses linear momentum and becomes diffusive under shortness of breath conditions ( $Q = 4$  Lpm). This is consistent with observations where nasal exhalation puffs extending straight out to about 60 cm have been reported with adult humans that exhale somewhat greater  $V_t$  under normal breathing conditions<sup>36</sup>.

When the nose and mouth are both open as in Fig. 3C, most of the exhalation emerges through the mouth, because of the relatively lower resistance offered by the wider and shorter oral passage compared with the nasal passage. The air flow emerges from the mouth at a higher elevation angle of  $36 \pm 2$  degrees in Fig. 3C compared with when it emerges from the nose as in Fig. 3B, under otherwise similar conditions.

A greater speed of  $1.64 \pm 0.08$  m/s, and greater distance of  $0.51 \pm 0.01$  m is reached before the exhalation puff becomes diffusive when exhaling through the mouth compared with the nose. Because exhalations through the mouth are at a higher elevation angle, they reach a higher elevation compared to nasal breathing, further increasing the risk to those working near the patient.

To illustrate the dynamics, a backlit image of the exhalation puff emerging through the nose past the nasal cannula is shown in Fig. 4A (from SI Movie 4), and the contained vortex dynamics made visible by the cross-sectional laser imaging in Fig. 4B (from SI Movie 5). Here the data corresponding to a mid-range of flow rates using  $Q = 4$  Lpm is shown. To illustrate the corresponding spread of the exhalation near the manikin, Fig. 4C shows the corresponding exhalation density averaged over several breath cycles projected in the vertical plane. The exhalation is observed to spread conically forward and concentrate in a single fast moving main puff as it mixes with the air in the room, loses momentum, and becomes diffusive.

It can be noted that some secondary puffs exist around the nose depending on exactly how the nasal cannula is mounted in the nose. Because of the presence of these puffs, the exhalation density does not decay as rapidly as the inverse square of the distance from the nose/mouth of the patient in all directions in front of the patient. Thus, the puffs end up increasing the concentration of exhalations directly above and in front of the face of a supine patient in a more focused region.

#### B. Dispersal through Simple O<sub>2</sub> Mask

A simple O<sub>2</sub> mask emits three puffs in total, each in different directions. Fig. 5A-C shows that a simple O<sub>2</sub> mask redirects the exhalations largely through the vents on either side of the device, and to a smaller degree from the gap between the mask and the bridge of the nose. Here the data corresponding to the mid-range of flow rates using  $Q = 8$  Lpm is shown, and the corresponding Movies 6,7 show examples from Fig. 5A,B, respectively. Very little escapes from around the chin because the O<sub>2</sub> mask fits relatively tightly in that area. The exhalation puffs from the vents on either side of the simple O<sub>2</sub> mask appear broader and have a rounder shape compared with the puffs coming from the nasal cannula. Vortex structures extending along lines starting at each of the vents are also evident from the cross section laser imaging on either side of the mask in Fig. 5B,

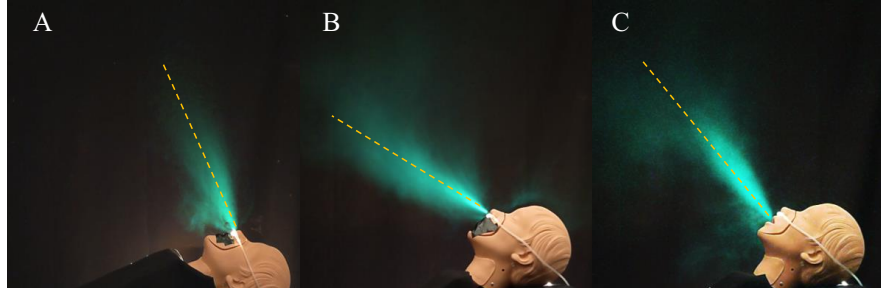


Figure 3. The time averaged exhalations emerging from the nose of a medical manikin fitted with a nasal cannula when the head rests flat (A), and while it is on a bed propped at 45 degrees (B), and when exhaling through the mouth (C), under shortness of breath conditions ( $V_t = 350$  mL at  $f = 20$  bpm;  $Q = 4$  Lpm). The aerosol-laden exhalation is visualized with back lighting and rendered with artificial cyan coloring. The primary exhalation air flow is observed to spread conically with principal direction indicated by the dashed line with elevation angle  $\theta = 60 \pm 0.5$  degrees (A),  $19.3 \pm 0.5$  degrees (B), and  $56 \pm 1$  degrees (C). Multimedia view

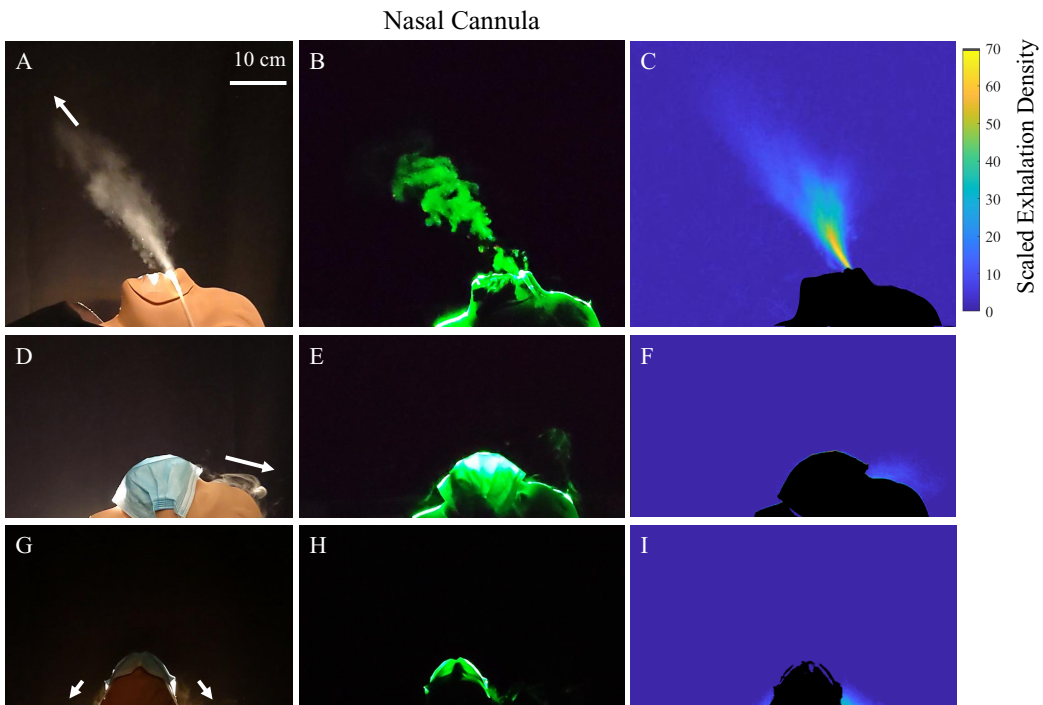


Figure 4. Exhalation puffs emerge from the nose while wearing a nasal cannula with an oxygen delivery flow rate of  $Q = 4$  Lpm. (A-C) Sagittal view with nasal cannula. (D-F) Sagittal view with cannula and surgical mask on top. Some exhalations are redirected towards the nose bridge of the patient. (G-I) Transverse view with cannula and surgical mask on top. The exhalation puffs are redirected mostly downward away from the face of a caregiver as indicated by the arrows. The cross-sectional laser illumination in (B) reveals repeating pattern of swirling vortices signifying considerable linear momentum in the exhalation puffs emerging past the unmitigated nasal cannula (see corresponding movie). The time-averaged projected exhalation density exhalation scaled by the mean density  $\rho_m = 0.71 \times 10^{-3}$  kg/m<sup>2</sup> if the exhalation were uniform is shown by the color bar. Multimedia view

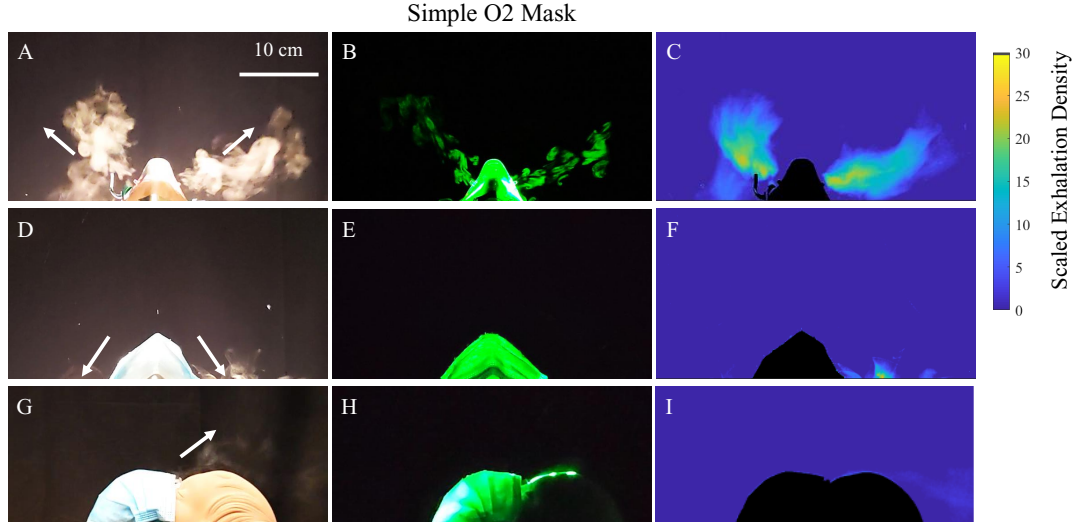


Figure 5. Exhalation puffs emerge from the nose while wearing a simple O<sub>2</sub> mask with an oxygen delivery flow rate of  $Q = 8$  Lpm. (A-C) Transverse view with simple O<sub>2</sub> mask. (D-F) Transverse view with simple O<sub>2</sub> mask and surgical face mask placed on top. With a surgical mask on top, the puffs are redirected mostly downward away from the face of a caregiver as indicated by the arrows. (G-I) Sagittal view with simple O<sub>2</sub> mask and surgical face mask placed on top. Some of the exhalation also escapes from the nose bridge region. Note the repeating vortex structures along the puff emerging from the simple O<sub>2</sub> mask vents indicates significant exhalation momentum in (B). The time-averaged projected exhalation density scaled by the mean density  $\rho_m = 1.41 \times 10^{-3}$  kg/m<sup>2</sup> if the exhalation were uniform is shown by the color bar. Multimedia view

and the associated Movie 7. Just as in the exhalation past the nasal cannula, these swirling vortices are associated with significant linear momentum when a fast-moving fluid enters a still region. The distance the puffs extend out is approximately  $0.29 \pm 0.02$  m. These slightly lower distances compared to the nasal cannula are consistent with the formation of two dominant puffs versus one dominant puff as in the nasal cannula.

The average exhalation density reached over an entire breathing cycle is shown in Fig. 5C, looking down from the top of the head, or, the transverse view. While not as elevated as in the case of the nasal cannula, the exhalation density resulting from the puffs emerging from the vents in the simple O<sub>2</sub> mask are pointed directly where caregivers typically stand while giving care to a supine patient. Because of the presence of the puffs, the exhalation density in the case of the simple O<sub>2</sub> mask does not decay as rapidly as the inverse of the square of the distance from the face, but rather is concentrated in particular directions. It can be further observed from the color bar that the exhalation densities reached near the vicinity of the head are comparable to those reached near the vicinity of the head while wearing a nasal cannula shown in Fig. 4C.

Thus, the exhalation density around an unmiti-

gated oxygenation device is greater in different directions in relation to the head because of the presence of the puffs in each device versus if the exhalations were diffusing out uniformly from the device. We further quantify the resulting spatial distribution and concentration levels and effect of oxygenation rates next, before examining the effect of placing a surgical mask.

### C. Time-averaged exhalation cone analysis

When an exhalation puff from the mouth or nose enters the relatively quiescent air it spreads out in a cone in the time-averaged images as shown in Fig. 6. The Reynolds number, used to characterize the fluid flows, is given by  $Re = \frac{DU}{\nu}$ , where  $\nu = 1.6 \times 10^{-5}$  m<sup>2</sup>/s is the kinematic viscosity for air,  $D$  is the jet diameter, and  $U$  is its speed<sup>37</sup>. Assuming,  $D \approx 2$  cm, and  $U \approx 1.5$  m/s,  $Re \approx 2000$ . The flows corresponding to these  $Re$  are considered turbulent, consistent with the observation of vortex swirl patterns seen in the exhalation puffs entering relatively still air while wearing the nasal cannula (Fig. 4, SI Movies 1-3) or the simple O<sub>2</sub> mask (Fig. 5, SI Movies 6 and 7). It must be noted here that the observed repeated struc-

tures are not simply a result of periodic breaths interacting with each other, but are likely a result of shear instability<sup>13,19,37,38</sup>. A more in depth study is needed to confirm this hypothesis.

The measured cone angle  $\phi_c$  of the turbulent exhalation puffs are shown in Fig. 6. The measured angles are observed to be nearly constant across the oxygenation flow rates, indicating that the cross-section of the puffs are not affected by the oxygen flowing from the nasal cannula in the nose. This is also consistent with the near constant percentage of exhalation observed to move upward and forward as a function of  $Q$  in the nasal cannula. When a fast moving jet enters a still fluid from a uniform conduit, there exists a universal value of  $23.6^\circ$  in which the fluid spreads based on the law of similarity<sup>31,38</sup>. In the case when the manikin is not wearing an oxygen therapy device, the cone angle is approximately  $23.5^\circ$  through the nose and  $23.3^\circ$  through the mouth. The measured cone angles while wearing the nasal cannula are similar to this value with  $\phi_c = 26.4^\circ \pm 1.5^\circ$  for nasal breathing, and  $\phi_c = 26.6^\circ \pm 1.5^\circ$  for mouth breathing considering the error in measurements. Thus, we deduce that the flow around its stem appears to lead to a slightly larger cone angle compared to the universal value for a jet. By contrast, the observed cone angles  $\phi_c \approx 29.5^\circ$  in the case of the simple O<sub>2</sub> mask is somewhat higher compared with the nasal cannula.

While the time-averaged density of the exhalations decreases uniformly away from the central axis in Fig. 6, one can obtain a simple estimate of the increased risk to exposure assuming that the exhaled aerosols are uniformly distributed within  $\phi_c$ . Then, this focusing of the exhalation puffs in the conical region implies that the concentration of aerosols is given by the ratio of the area of the hemisphere above the patient and corresponding area of the spherical cap corresponding by  $\phi_c$  at the same distance  $r$  from the source (see Fig. 6C). Then, from the area of the spherical cap is  $A_c = 2\pi r^2(1 - \cos(\phi_c/2))$ , and the area of the hemisphere  $A_{hs} = 2\pi r^2$ , we get the relative aerosol concentration ratio  $\chi_r = 1/(1 - \cos(\phi_c/2))$ . In the case of the nasal cannula, we accordingly find the concentration ratio  $\chi_r$  to be approximately 38 times compared to what may be expected if emerging uniformly. In the case of the simple O<sub>2</sub> mask we observe that the exhalations emerge mostly in two evenly distributed exhalation puffs. Then, considering the mid-range of observed  $\phi_c \approx 29.5^\circ$  in the case of the simple O<sub>2</sub> mask, one can estimate the concentration  $\chi_r$  to be approximately 15 times higher in the two focused exhalation regions compared with when emerging uniformly in all di-

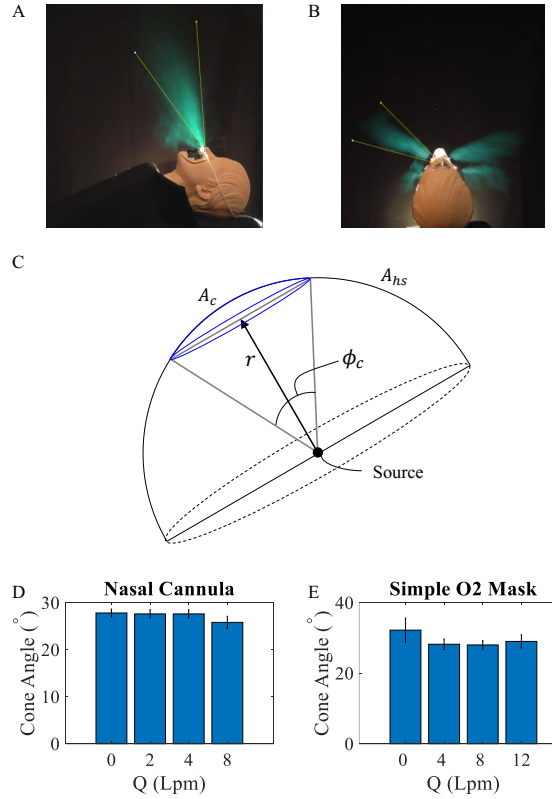


Figure 6. Representative time averages showing the spread of the exhalation puffs in conical regions for the (A) sagittal view of the nasal cannula and (B) transverse view of the simple O<sub>2</sub> mask. The aerosol-laden exhalation is visualized with back lighting and rendered with artificial cyan coloring. (C) A schematic of the conical exhalation regions with high aerosol concentration relative to a hemisphere around the source. The measured exhalation cone angles  $\phi_c$  are observed to be essentially constant across the oxygenation flow rates  $Q$  for (D) nasal cannula and (E) simple O<sub>2</sub> mask. The data for  $Q = 0$  Lpm was taken for reference.

rections above the face of the patient.

This estimate assumes the density is uniformly distributed in the spherical cap bounded by the conical envelope, whereas the concentrations are even more narrowly peaked around the central axis within the conical region denoted by the arrows in Fig. 6. This approach provides a lower bound for the aerosol concentration near the patient's head. The actual concentrations locally can be even higher in space and time. These measurements and estimates thus highlight the need to mitigate risk posed by the direct path of the exhalation puffs.

#### IV. EXHALED PUFF REDIRECTION WITH SURGICAL MASK COVER

Figure 4D-I and Figure 5D-I shows the effect of placing a loosely fitted surgical face mask over an oxygenation device under otherwise similar conditions. The term "loosely fitted" refers to the fact that the face mask is clasped behind the manikin ears as designed to be used. During the breathing cycle, no significant deformation in the face mask material was observed, which indicates the lack of a tight sealed fit and indicates ease of breathing. Measuring the pressure in the breathing apparatus, we find no measurable difference whether a surgical mask is placed on, or not, to within measurement fluctuations from breath to breath of  $\pm 0.2 \text{ cm H}_2\text{O}$  or  $\pm 19.6 \text{ Pa}$ . Orthogonal views are shown to give a complete picture of the exhalation dispersal with this mitigation strategy. Here, the surgical mask was placed loosely on top of the oxygenation device to limit the effect on the work of breathing<sup>39</sup>. Thus, the primary objective is to deflect the exhalation puffs, rather than to filter them as in the N95 mask. From these side-by-side images, and the associated movies in Figures 4 and 5 (Multimedia view) over the range of oxygen flow rates used, we observe that the exhalation puffs are reduced and get deflected behind the manikin face.

Contrasting the unmasked and masked cases in Fig. 4 and Fig. 5, the addition of the surgical mask atop the oxygenation devices works to dissipate the initial momentum of the exhaled air, besides redirecting the exhalation puffs coming through the devices downward. Thus, health workers who would otherwise be in the direct pathway of the exhalation when providing care to a supine patient, will not face the direct exhalation puff. Rather, the exhalation will be redirected downward to be nearly orthogonal to the directional line between a patient and their care-giver, significantly alleviating the direct exhalation concentration above the mask.

##### A. Spatial distribution assessment

The backlit exhalation movies are further analyzed using the MATLAB image processing toolbox. We first conducted background subtraction to isolate the intensity of the illuminated aerosols. The mean measured light intensity, corresponding to the light scattered by the aerosol-laden exhalations after an exhalation cycle, is mapped to the mean projected exhalation density  $\rho_m$  in the measured frame encompassing the entire area over which exhalations are observed to reach in one breathing cycle. This mean density

is given by the mass of the exhaled volume of air  $V_t$  multiplied by the density of exhaled air  $\rho_a = 1.22 \text{ kg/m}^3$ , and divided by the area of the frame. This density corresponds to the density if the exhalation were uniformly spread, and is used to assess the relative risk of higher dose of virus bearing exhalations in a certain area because of the puffs, in comparison to a scenario in which the exhalations spread out uniformly. The distance of the exhalation puffs is identified by plotting the scaled exhalation density along the observed puffs, and then identifying the point where the density has decreased to be within 50% of the mean density.

In order to quantify the degree of mitigation, Fig. 7A shows the angular exhalation density as a function of angle  $\theta$  around the manikin head as defined in the inset to Fig. 7A. Here the angular density is obtained by integrating the measured projected exhalation density (as in Fig. 4C and Fig. 4F) from the face out to the furthest distance where exhalations are observed to reach above the face. Both plots corresponding to the exhalations without, and with, the surgical mask fixed atop the oxygenation devices are shown. It can be observed that the large puff which travels upward and forward is clearly suppressed by the placement of the mask. The same angular exhalation density is calculated for a simple  $\text{O}_2$  mask using the views shown in Fig. 5C and Fig. 5F, and plotted in Fig. 7B. Two peaks are observed corresponding to the two principal puffs that emerge upward and outward from the vents of the simple  $\text{O}_2$  mask. As in the nasal cannula, clear suppression of the exhalation puffs is quantitatively observed with the surgical mask placed over the simple  $\text{O}_2$  mask.

To quantify the degree of mitigation with distance above the mask, we plot the exhalation density along the principal puffs in the unmasked cases in the nasal cannula and simple  $\text{O}_2$  mask in Fig. 7C and Fig. 7D, respectively. These directions also correspond to the angle at which the maximum in the angular exhalation density occurs in each device in Fig. 7A and Fig. 7B. The exhalation density is observed to become significantly lower with the surgical mask on. Comparing the values without and with surgical mask in Fig. 7C,D, the exhalation density at  $r = 15 \text{ cm}$  can be observed to be at least 30 times smaller in each device. These measurements can be observed to be consistent with the estimates of unmitigated aerosol dispersal in conical regions above the manikin discussed in Section III C.

Thus, adding a surgical mask even loosely over either oxygen therapy devices can be seen to quantitatively reduce direct exposure to high exhalation aerosol concentrations created by exhalation puffs

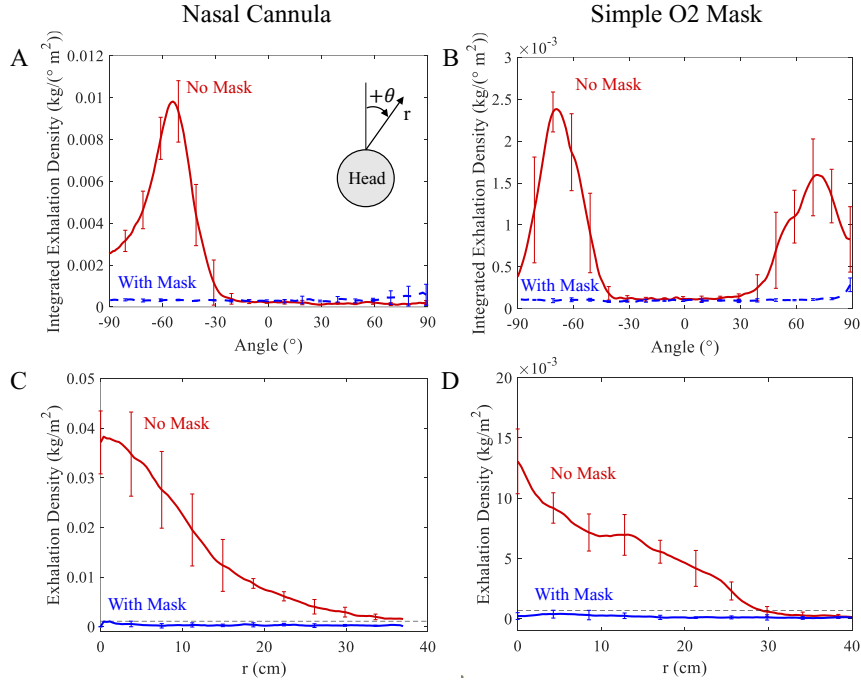


Figure 7. The angular integrated dispersal exhalation intensity is suppressed when a surgical mask is placed on top in both devices (A,B). The distance over which the puffs reach is observed to be dramatically curtailed in both devices (C,D). The bars represent the range of values among five trials used to calculate the plotted averages. The exhalations travel up to 37 cm for the nasal cannula and 31 cm for the simple O<sub>2</sub> mask when unmitigated. The black dashed line represents the threshold value that is 50% greater than the mean exhalation density  $\rho_m$  used to determine the exhalation distance.

above the face.

### B. Dispersal mitigation with Oxygen flow rate

To quantify the degree of mitigation by a surgical mask with each oxygenation device, the percentage of exhalations observed above the face without and with a surgical mask is obtained by integrating the measured exhalation density above the plane defined by the surgical mask over one exhalation cycle (roughly 6 seconds). Figure 8A and Fig. 8B show the degree of mitigation observed over the oxygen flow rates examined in the nasal cannula and simple O<sub>2</sub> mask, respectively, averaged over 5 independently measured breathing cycles in separate data runs. The percent of exhalations as a function of oxygen flow rates show no particular trend and can be considered more or less flat across the entire range, even while considering the small variations noted by the error bars from the five independent experiments. This is also consistent with the fact that the highly concentrated aerosol conical regions are absent after placement of the surgical mask, as in the nasal cannula exhalation

tion (Fig. 4C,F) and the simple O<sub>2</sub> mask exhalation (Fig. 5C,F), after placement of the surgical mask.

The average exhalation volume per minute given by the number of breaths per minute times the tidal volume, which is 7 Lpm under shortness of breath conditions, and 6 Lpm under normal breathing, are similar to  $Q$  in the case of the nasal cannula. However, if one considers that the majority of the exhalation occurs over a fraction of the breathing cycle, the momentum associated with the exhalation itself can be proportionally higher and can dominate the dispersal over the range of oxygen flow rates used. Using the surgical mask limits the exhalations from the puffs in the directions above the mask to about 10% of the total exhalation volume over the entire range of oxygen flow rates. While exhalations do escape from the sides downwards and may diffuse upwards (Fig. 4 and 5, 2nd & 3rd rows), this contribution to the exhalation with a surgical mask is significantly less compared with unmitigated exhalations.

Overall, a loosely fitted surgical mask over a nasal cannula, or simple O<sub>2</sub> mask, redirects exhalations downward and thus away from the faces of caregivers, while simultaneously reducing the volume and den-

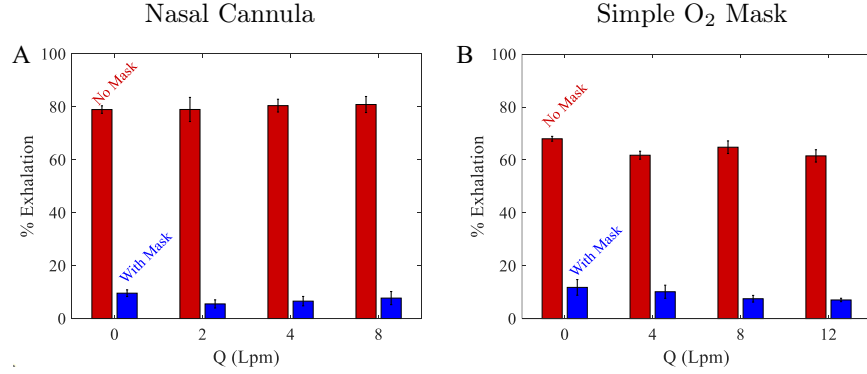


Figure 8. The percent of breath that is exhaled above the face without and with surgical mask as a function of flow rates for (A) the nasal cannula and (B) the simple O<sub>2</sub> mask. All cases have five trials.

sity of the exhalations reached above the patient. The surgical mask is only loosely placed to alleviate any concern for increased work of breathing, i.e. to deflect rather than filter the aerosols. The surgical mask is demonstrated to quantitatively reduce exhalation density concentration above the mask. By preventing the exhalations from being launched directly up, the placement of a mask can also suppress wider dispersal of the exhalations depending on the ventilation currents. It should be emphasized that our study pertains to a supine patient, and does not apply to patients in the prone position.

## V. CONCLUSIONS

We have constructed a reproducible exhalation system which enables us to quantitatively demonstrate that significant exhalation puff dynamics exist with either a nasal cannula or simple O<sub>2</sub> mask commonly used in treating COVID-19 and other respiratory disease patients. The exhalations are observed to be concentrated in conical regions in front of the patient as the exhalations move with significant linear momentum before becoming diffusive.

When using the nasal cannula, the exhalations move linearly to significant distances and split slightly around the stem of the device while nasal breathing. The exhalations are angled slightly upwards in comparison to the free breathing case, and its angle varies somewhat depending on exactly how the nasal cannula is placed. Mouth breathing angles the exhalations relatively higher compared with nasal breathing with a nasal cannula, leading to greater dispersal distances. By contrast, the simple O<sub>2</sub> mask has upward and lateral puffs that travel out to similar distance from the mask vents on both sides, and

one smaller upward puff from the bridge of the nose. However, the exhalations are launched higher and thus spread further as they slowly disperse depending on the air flow within the room. In all cases, the aerosol concentration is found to be many times higher compared to assuming that the exhalations spread uniformly above the patient.

Mitigation is demonstrated by reducing exhalation puffs by using a surgical mask over the oxygenation devices. The mask is loosely placed to redirect rather than filter exhalations. In all cases the exhalations are directed downwards and away from the faces of health care workers working around the patient's head. The surgical mask is found to limit the direct exhalations to about 10 % (compared to when no mask is placed) above the face over the entire range of oxygen flow rates used in either device. While the exhaled aerosols spread out over time, this transport is diffusive and can be managed with proper ventilation systems in place. The surgical mask reduces and redirects the exhalations while wearing the nasal cannula and the simple O<sub>2</sub> mask by dissipating the momentum of the exhalations.

In current practice, there is generally no mitigation in place, on the patient side, should they sneeze or cough while receiving care. The placement of the mask can also reduce the larger aerosols and droplets expired when the patient speaks, coughs or sneezes, if not totally eliminate them<sup>15,35,36,40</sup>. Thus, our study demonstrates the efficacy of placing a surgical face mask over the nasal cannula and the simple O<sub>2</sub> mask in reducing exhalation exposure risk to caregivers treating patients with COVID-19, and other infectious respiratory diseases.

## ACKNOWLEDGMENTS

We thank Chris Blanker, Sujata Davis, Germano Iannacchione, and Catherine Taylor for advice, discussions, and help with study. This work was supported by U.S. National Science Foundation COVID-19 RAPID Grant No. DMR-2030307.

## DATA AVAILABILITY STATEMENT

The data that support the findings of this study are available within the article.

## REFERENCES

- <sup>1</sup>Maire P Shelly and Peter Nightingale. Respiratory support. *BMJ*, 318(7199):1674–1677, 1999.
- <sup>2</sup>AS BaHamman, TD Singh, R Gupta, and SR Pandi-Perumal. Choosing the proper interface for positive airway pressure therapy in subjects with acute respiratory failure. *Respiratory Care*, 63(2):227–237, 2018.
- <sup>3</sup>Martin Z. Bazant and John W. M. Bush. A guideline to limit indoor airborne transmission of covid-19. *Proceedings of the National Academy of Sciences*, 118(17), 2021.
- <sup>4</sup>MJ Tobin. *Principles and Practice of Mechanical Ventilation*. McGraw-Hill Education, 2010.
- <sup>5</sup>BR Oâ€™driscoll, LS Howard, and AG Davison. Bts guideline for emergency oxygen use in adult patients. *Thorax*, 63(Suppl 6):vi1–vi68, 2008.
- <sup>6</sup>DS Hui, BK Chow, SS Ng, LCY Chu, SD Hall, T Gin, JJY Sung, and MTV Chan. Exhaled air dispersion distances during noninvasive ventilation via different respiration face masks. *Chest*, 136:998–1005, Dec 2009.
- <sup>7</sup>JA McGrath, A O’Sullivan, G Bennett, C O’Toole, Joyce M, MA Byrne, and RM MacLoughlin. Investigation of the quantity of exhaled aerosols released into the environment during nebulisation. *Pharmaceutics*, 11:75, 2019.
- <sup>8</sup>D Brunk. Noninvasive ventilation: Options and cautions for patients with covid-19. *Medscape*, Sept 2020.
- <sup>9</sup>JB Fink, S Ehrmann, J Li, P Dailey, P McKernan, C Darquenne, AR Martin, B Rothen-Rutishauser, PJ Kuehl, S Häussermann, R MacLoughlin, GC Smaldone, B Muellinger, TE Corcoran, and R Dhand. Reducing aerosol-related risk of transmission in the era of covid-19: An interim guidance endorsed by the international society of aerosols in medicine. *J Aerosol Med Pulm Drug Deliv*, 33:300–304, 2020.
- <sup>10</sup>CR MacIntyre and AA Chughtai. Facemasks for the prevention of infection in healthcare and community settings. *BMJ*, 350, 2015.
- <sup>11</sup>D Tsilingiris, M Papatheodoridi, and CJ Kapelios. Providing evidence on the ongoing health care workersâ€™ mask debate. *Intern Emerg Med*, 15:773â€“777, 2020.
- <sup>12</sup>L Bourouiba, E Dehandschoewercker, and JWM Bush. Violent expiratory events: On coughing and sneezing. *Journal of Fluid Mechanics*, 745:537–563, 2014.
- <sup>13</sup>M Abkarian, S Mendez, N Xue, F Yang, and HA Stone. Speech can produce jet-like transport relevant to asymptomatic spreading of virus. *Proc Nat. Acad Sci USA*, 117(41):25237–25245, 2020.
- <sup>14</sup>S Verma, M Dhanak, and J Frankenfield. Visualizing the effectiveness of face masks in obstructing respiratory jets. *Physics of Fluids*, 32(6):061708, 2020.
- <sup>15</sup>B Chang, RS Sharma, T Huynh, and A Kudrolli. Aerial mucusalivary droplet dispersal distributions with implications for disease mitigation. *Phys. Rev. Research*, 2:043391, Dec 2020.
- <sup>16</sup>M Staymates. Flow visualization of an n95 respirator with and without an exhalation valve using schlieren imaging and light scattering. *Phys Fluids*, 32(11):111703, 2020.
- <sup>17</sup>Prateek Bahl, Charitha M. de Silva, Abrar Ahmad Chughtai, C. Raina MacIntyre, and Con Doolan. An experimental framework to capture the flow dynamics of droplets expelled by a sneeze. *Experiments in Fluids*, 61(8):176, Aug 2020.
- <sup>18</sup>Prateek Bahl, Shovon Bhattacharjee, Charitha de Silva, Abrar Ahmad Chughtai, Con Doolan, and C Raina MacIntyre. Face coverings and mask to minimise droplet dispersion and aerosolisation: a video case study. *Thorax*, 2020.
- <sup>19</sup>Ali Khosronejad, Seokkoo Kang, Fabian Wermelinger, Petros Koumoutsakos, and Fotis Sotiropoulos. A computational study of expiratory particle transport and vortex dynamics during breathing with and without face masks. *Physics of Fluids*, 33(6):066605, 2021.
- <sup>20</sup>Chong Shen Ng, Kai Leong Chong, Rui Yang, Mogeng Li, Roberto Verzicco, and Detlef Lohse. Growth of respiratory droplets in cold and humid air. *Physical Review Fluids*, 6(5):054303, 2021.
- <sup>21</sup>Kai Leong Chong, Chong Shen Ng, Naoki Hori, Rui Yang, Roberto Verzicco, and Detlef Lohse. Extended lifetime of respiratory droplets in a turbulent vapor puff and its implications on airborne disease transmission. *Physical review letters*, 126(3):034502, 2021.
- <sup>22</sup>Liangyu Wu, Xiangdong Liu, Feng Yao, and Yongping Chen. Numerical study of virus transmission through droplets from sneezing in a cafeteria. *Physics of Fluids*, 33(2):023311, 2021.
- <sup>23</sup>M Klompas, MA Baker, C Rhee, R Tucker, K Fiumara, D Griesbach, C Bennett-Rizzo, H Salmasian, Ri Wang, N Wheeler, GR Gallagher, AS Lang, T Fink, S Baez, S Smole, L Madoff, E Goralnick, A Resnick, M Pearson, K Britton, J Sinclair, and CA Morris. A sars-cov-2 cluster in an acute care hospital. *Ann Intern Med*, 2021. PMID: 33556277.
- <sup>24</sup>JA Razzak, JA Bhatti, MR Tahir, and O Pasha-Razzak. Initial estimates of covid-19 infections in hospital workers in the united states during the first wave of pandemic. *PLOS ONE*, 15(12):1–9, 12 2020.
- <sup>25</sup><https://vapotherm.com/covid-19/>.
- <sup>26</sup>J Li, JB Fink, AA Elshafei, Laurel M Stewart, HJ Barbian, SH Mirza, L Al-Harthi, D Vines, and S Ehrmann. Placing a mask on covid-19 patients during high-flow nasal cannula therapy reduces aerosol particle dispersion. *ERJ Open Res*, 2020.
- <sup>27</sup>SH Cataldo, BP Harvey, and MJ Pedro. Comparative efficacy of aerosolized particle filtration by non-invasive ventilation modalities: Simulation of sars-cov-19 transmission. *Am J Biomed Sci & Res*, 9:MS.ID.001460, Aug 2020.
- <sup>28</sup>Gabriel Enrique Mejia-Terrazas and Eunice López-Muñoz. Supplemental oxygen in surgical patients with covid-19. *Journal of anesthesia*, 34(6):958–958, 2020.
- <sup>29</sup>Yusuke Matsui, Tomonori Takazawa, Akihito Takemae, and Shigeru Saito. Does a surgical mask improve oxygenation in covid-19 patients? *JA clinical reports*, 7(1):1–3, 2021.
- <sup>30</sup>Asad Khan, William T. McGee, and et al. Baystate medical center national O2 mask usage clinical care survey. Survey data downloaded January, 23,

2021 at <https://www.surveymonkey.com/results/SM-CDRTMHCZ7> (to be published).

<sup>31</sup>G. N. Abramovich. *General Properties of Turbulent Jets*, pages 3–49. 2003.

<sup>32</sup>R Chou, T Dana, R Jungbauer, C Weeks, and MS McDonagh. Masks for prevention of respiratory virus infections, including sars-cov-2, in health care and community settings. *Annals of Internal Medicine*, 173(7):542–555, 2020. PMID: 32579379.

<sup>33</sup>Sadeq A Quraishi, Lorenzo Berra, and Ala Nozari. Indoor temperature and relative humidity in hospitals: Workplace considerations during the novel coronavirus pandemic. *Occupational and Environmental Medicine*, 77(7):508–508, 2020.

<sup>34</sup>Richard E Fairfax. Osha memorandum: Reiteration of existing osha policy on indoor air quality: Office temperature/humidity and environmental tobacco smoke | occupational safety and health administration, 2003.

<sup>35</sup>JW Tang and GS Settles. Coughing and aerosols. *New England Journal of Medicine*, 359(15):e19, Oct 2008.

<sup>36</sup>JW Tang, AD Nicolle, CA Klettner, J Pantelic, L Wang, A Bin Suhaimi, AYL Tan, GWX Ong, R Su, C Sekhar, DDW Cheong, and KW Tham. Airflow Dynamics of Human Jets: Sneezing and Breathing - Potential Sources of Infectious Aerosols. *PLoS ONE*, 8(4):1–7, 2013.

<sup>37</sup>DJ Tritton. *Physical Fluid Dynamics*. The Modern University in Physics Series. Springer Netherlands, 2012.

<sup>38</sup>B Cushman-Roisin and JM Beckers. *Introduction to Geophysical Fluid Dynamics - Physical and Numerical Aspects*. Academic Press, 2005.

<sup>39</sup>Rebecca H Haraf, Mark A Faghy, Brian Carlin, and Richard A Josephson. The physiological impact of masking is insignificant and should not preclude routine use during daily activities, exercise, and rehabilitation. *Journal of cardiopulmonary rehabilitation and prevention*, 41(1):1, 2021.

<sup>40</sup>ZY Han, WG Weng, and QY Huang. Characterizations of particle size distribution of the droplets exhaled by sneeze. *J R Soc Interface*, 10(88):20130560, Nov 2013.